Roumanian Biotechnological Letters *Vol. 9, No. 5, 2004, pp 1853-1870*

ORIGINAL PAPER

Radiation effects on cell proliferation

Received for publication, September 8, 2004
Accepted October 20, 2004

I. BARAN[1,2], C. LOPRESTI[2], F. MUSUMECI[2,3], G. PRIVITERA[2], S. PRIVITERA[2], A. SCORDINO[2,3], S. TUDISCO[2], V. BARAN[2,4], G.A.P. CIRRONE[2], L.RAFFAELE[2], L.VALASTRO[2]

[1]*Biophysics Dept., Univ. of Medicine and Pharmacy "Carol Davila", Bd. Eroii Sanitari 8, 76241 Bucharest, Romania*

[2]*Laboratori Nazionali del Sud, Istituto Nazionale de Fisica Nucleare, via S. Sofia 62, I-95123 Catania, Italy*

[3]*Dipartimento di Metodologie Fisiche e Chimice pe l'Ingegneria, Unita INFM, Universita di Catania, viale A. Doria 6, I-95125 Catania, Italy*

[4]*Dept. of Theoretical Physics and Mathematics, Physics Faculty, University of Bucharest, and NIPNE-HH, Bucharest, PO Box MG-6, Magurele, Romania*

Keywords: cell proliferation, gamma rays, protons, delayed luminiscence, DNA damage

Abstract

We quantify several effects of γ- and proton-radiation on asynchronous cell cultures of the wild-type S. cerevisiae. At 200 Gy, γ rays produce DNA lesions that arrest cells at the G_2/M checkpoint a longer time than do protons. The relative yield of lethal damage (DNA double strand breaks – dsbs – that cannot be repaired during cell cycle progression) appears closely similar in both radiation types, but injury is more severe in the proton-radiation case: the relative yield of irreparable alterations (dsbs that cannot be repaired neither in G_0 stationary phase nor during cell cycle progression) is 0.31 with protons as compared to 0.001 in the case of γ rays. We combined the methylene-blue exclusion test with the colony-forming ability test and obtained that irradiated cells carrying lethal damage die on average during the third division-cycle. Onset of radiation-induced cell death appears with a lag of 220 min. after γ-irradiation, and of 155 min. after proton-irradiation. The radiation effects on the delayed luminescence characteristics are evidenced through variations in the total yield of the light emitted by cells and the kinetics of light decay. The results reveal that cells after irradiation enter a specific phase, characterized by increased number of excited states that emit red (645 nm) light following laser excitation and increased fraction of states that decay at high rate.

Introduction

Cell cycle progression is transiently arrested in response to DNA damage, inhibition of DNA replication or incorrect assembly of the mitotic spindle, which may be induced by ionizing radiations or other physical/chemical agents. The cellular mechanisms involved in this delaying effect are precisely coordinated at specific checkpoints, allowing time for damage repair [1, 2]. Checkpoints are designed for two primary purposes: to prevent cell division when DNA is damaged or DNA replication is interrupted, and to regulate repair systems that help cells to survive replicational stress. Three responses have been characterized in budding yeast, which are known as the G_1/S, intra-S and G_2/M DNA damage checkpoints, depending on the cell cycle phase at which DNA alterations occur.

DNA damage occurring in the G_1 phase induces delay in bud emergence and entry into S-phase through induction of the G_1 checkpoint response. The S-phase checkpoint is activated

by DNA damage detected during S-phase, as well as incomplete DNA replication, and coordinates DNA replication with DNA repair capacity. The G_2 checkpoint allow DNA damage repair that was not completed during S-phase, or can respond to DNA damage or cytoskeletal disruptions that arise during G_2. The mitotic checkpoint delays anaphase onset when chromosomes fail to align correctly at the metaphase plate. If DNA damage is not repaired in a limited time at the G_2 or M checkpoint stage, the cells pass defectively to the next cell cycle stage, in a process termed adaptation [3] which can lead directly to genomic instability. In yeast cells the time spent at various checkpoints depends on the cell cycle phase and increases in the order $G_1/S/G_2$. The maximal time allowed for G_1 repair is 1 hour, while for G_2 repair is 10 hours [2].

We used two type of ionizing radiation, protons and γ rays, and investigated the radiation effects on cell proliferation for a fixed, high dose of 200 Gy. In addition to determinations of surviving cell fraction, we quantified the relative yield of irreparable DNA double strand breaks, the extent of cell accumulation at the G_2/M checkpoint, as well as the onset and rate of radiation-induced cell death following irradiation.

By combining the methylene-blue inclusion test of dead cells with the colony-forming ability test of surviving cells we obtain that irradiated cells that carry lethal damage die on average during the third division-cycle. This result comes in perfect agreement with that obtained from studies on X-rays irradiated yeast cells, where it has been concluded that a single cell producing at least a micro-colony of five cells is eventually able to form a colony and thus can be considered a survivor [4]. That means the division probability of cells to go from generation zero to three corresponds to the survival curve of the colony-forming ability test, or, equivalently, cells unable to divide three times do not survive irradiation.

All these effects were correlated with the variations observed in the properties of the delayed luminescence (DL) of yeast cells. The DL of solid state systems has been studied over the last decades [5]. It has been found in these systems that the DL phenomenon, different from the fluorescence process, is generated by excitation and subsequent decay of collective states, and that it disappears if these states are inhibited.

As recently highlighted [6] the DL of biological systems shows noticeable analogies with that of solid state systems and this fact suggests that the former could be explained by the same mechanism. In this case the collective states can exist as excitons or molecular solitons in the one-dimensional chains that constitute the cytoskeleton.

Materials and Methods

Cell cultures

Wild-type *Saccharomyces cerevisiae* yeast cells were grown overnight in rich glucose medium YPD (composed of 2% glucose, 1% yeast extract and 2% bactopeptone) at 30°C. Cells were brought to logarithmic phase by transfer to fresh YPD at a starting density of 5×10^6 cells/ml and allowed to reach $\cong 30\times10^6$ cells/ml.

Cell suspensions were transferred onto closed Petri dishes, equilibrated on ice, and irradiated at 0°C, with 200 Gy of either accelerated protons or γ rays. Control cells were subjected to the same treatment as irradiated cells except that they were kept outside the irradiation room.

Clinical proton beams accelerated by the superconducting cyclotron at the LNS-INFN, Catania (Italy) were used for proton-irradiation at a dose rate of 11.76 Gy/min. The proton beams were modulated to give uniform distribution of the absorbed dose. The proton energy

was 54.12 MeV at the entrance, and 15.43 MeV upon exit from the Petri dish. A plane-parallel advanced PTW 34045 Markus ionization chamber was adopted as reference dosimeter in the proton beam. The dose measurements were performed in a water phantom, according to International Atomic Energy Agency (IAEA) TRS 398. The absorbed dose to water per monitor unit (cGy/M.U.) is measured at isocenter, at the depth corresponding to the middle of the modulated beam, with the reference circular collimator (diameter=25 mm).

Clinical photon beams, available at the Radiological Institute of Catania University (Italy) were used for γ-irradiation. Here, a linear accelerator (Orion GE) produces a bremsstrahlung spectrum with photon energies < 5 MeV. The dose rate was 3.33 Gy/min. The calibration of the photon beam was performed by placing a cylindrical ionization chamber (Farmer 1384 by PTW) in a PMMA (PolyMethylMethAcrylate) phantom. The irradiation set-up, according to the American Association Physics in Medicine (AAPM) TG 21, was: field size 10x10 cm^2, Farmer chamber placed in a PMMA phantom at 5 cm water depth (corresponding to 4.4 cm PMMA), distance photon beam source to Farmer chamber 105 cm, distance photon beam source to phantom surface 100.6 cm.

After irradiation, cells were collected by centrifugation (1500 g, 2 min.), re-suspended in yeast nitrogen base without amino acids at a final concentration of $\cong 80\times10^6$ cells/ml and the resulting suspension was divided as follows: 0.1 ml used for immediate plating, 0.75 ml used for DL measurements, 0.1 ml used for photo-recordings, 0.11 ml transferred into 25 ml phosphate buffer saline (PBS) with antibiotic (culture DP), and ~10 ml diluted ~33 times in YPD to a final concentration $\cong 2.5\times10^6$ cells/ml (culture K). Suspensions DP and K were kept at 30°C with continuous agitation. At various moments samples were removed from culture K and adequately prepared for various investigations (DL measurements, dead cell test, photo-recordings).

After 3-5 days, cells in culture DP were counted and used for delayed plating, following the same procedure as for immediate plating.

For immediate plating, cells were sonicated for 30 s, then serial dilutions were made and samples containing 200 to 700 cells in YPD were spread on YPD agar plates, which were incubated at 30°C for 3 days. Colonies were then counted and survival of irradiated cells was calculated by averaging the ratios: no. of colonies (irradiated)/no. of colonies (control), obtained with the same number of plated cells.

For both YPD agar plates and PBS suspensions, the antibiotics used were: gentamycine 30 μl in 100 ml medium, and cloranphenycole 50 μg/ml.

Cell count was performed with the use of a Thoma haemocytometer, after appropriate dilution and brief (25-30 s), low power sonication. Dead cells were detected by means of the methylene-blue method [7].

Cell density, viability and budding profiles were examined with a CCD camera Logitech QuickCam Pro 4000, connected to an Olympus CK30 phase contrast microscope, giving an 800X overall magnification. The selection criteria for budding profiles and cell cycle phase distributions were: unbudded cells for G_1, small-budded cells for S, medium-budded cells for early-to-middle-G_2 and large-budded cells for late-G_2-M phase [8].

Prior to DL measurements, cells were collected by centrifugation of a 5-10 ml culture aliquot and transferred at a final concentration $\sim 80\times10^6$ cells/ml cells into a minimal medium containing [7] 6.7 g/liter yeast nitrogen base without amino acids (Sigma-Aldrich) and 10 g/liter dextrose (prepared according to the manufacturer's protocol). 0.2 ml of the resulting culture were prepared for microscopic examination and 150 μl drops were used for DL measurements under aerobic conditions, at a temperature of 30 ± 0.5 °C.

Delayed Luminescence Spectroscopy

In order to measure the DL of cell cultures an improved version of the ARETUSA set-up was used. This equipment can detect single photons and has a very low background signal; moreover, it presents high efficiency in collecting the luminescence emitted by cell cultures, and a short time of delay between the end of the illumination pulse and the beginning of signal acquisition. The improvements concern mainly the possibility of performing a spectral analysis of the examined samples.

The optics of the system was planned bearing in mind the necessity of using samples of small dimensions and, in spite of that, to have signals well discriminated from the background and from the luminescence arising from other parts of the device itself. To satisfy these requirements samples with a volume of about 150 μl were chosen; in the case of cell cultures, this quantity was obtained by using a precision pipette. The samples, confined by surface strength in a hemispherical shape, were placed on the upper side of a horizontal quartz window. Under these conditions no container was necessary for the cell culture and the luminescence of the plastic or quartz cuvettes, generally used as sample containers, was removed. Nevertheless, in this configuration a fraction of the laser light is reflected by the drop-shaped sample inside the head of the measuring apparatus, inducing undesired luminescence effects. We prevent this effect by using a special filter (Lot-Oriel 57345), placed immediately under the lower face of the quartz window. In any case the background signal, originating from the device as well as from the culture medium with and without the chemical, was measured apart. This signal was, in intensity, of the order of few percent of the total one and was subtracted from the signal coming out from the samples.

As a light source a Nitrogen Laser (Laser Photonics LN 230C), characterized by a wavelength λ=337 nm, a 5 ns pulse width, an energy of 100±5 μJ/pulse, was chosen. The laser power was reduced, in some cases, to prevent the dimpling of photomultiplier.

In order to guarantee a uniform illumination of the whole hemispherical culture drop, the laser was connected to an optical fiber whose output, on the other termination, was threefold, with all three sub-terminals located around the drop at constant angles of 120° between their directions.

The spectral analysis has been performed by a set of seven broad band (about 80 nm FWHM) interferential filters (Lot-Oriel 57510 / 30 / 50 / 90 / 610 / 30 / 50) placed in a suitable wheel, between the sample and the photomultiplier.

A multi-alkali photomultiplier tube (PMT) (Hamamatsu R-7602-1/Q), selected for single photons counting, was chosen as a detector. To obtain a significant reduction of the intrinsic dark current the PMT was cooled down up to –30°C, using a circulating cold liquid in direct contact with its surface.

The detector was placed as close as possible to the sample so, from a geometrical point of view, the total efficiency of such an arrangement was of about 8%, an order of magnitude higher than obtained with most of the previous systems.

During the laser pulses a large quantity of photons (of the order of 10^{12}), diffused by the sample, will reach the photocathode within 1 ns, inducing irreversible damage of the photomultiplier. In order to prevent this effect and to guarantee a fast start of the signal acquisition, an electronic inhibition system, able to modify the voltage at the first two dynodes of the photomultiplier was carried out [9]. The time performances of this electronic gate permit, in principle, the start of the acquisition 10 □s after the illumination pulse. The detected signals are acquired by a Multi-channel Scaler (MCS) (Ortec MCS PCI), able to collect analogical or logical signals as a function of time, with a minimum dwell time of 200 ns.

Results

Normal cell growth

Normal cells grow in liquid YPD at 30°C with a mean doubling time of 90.2±4.3 min. (n=4). We estimated the cellular death rate with the methylene blue method, assuming that all dead cells at t<350 min. are exclusively mother cells present in culture at the moment of inoculation, t=0. The mean lifetime obtained from the best exponential fit to the data (see Fig. 1) is evaluated as 882 min., meaning that yeast cells die on average after nine-ten divisions, which furthermore supports the approximation made above.

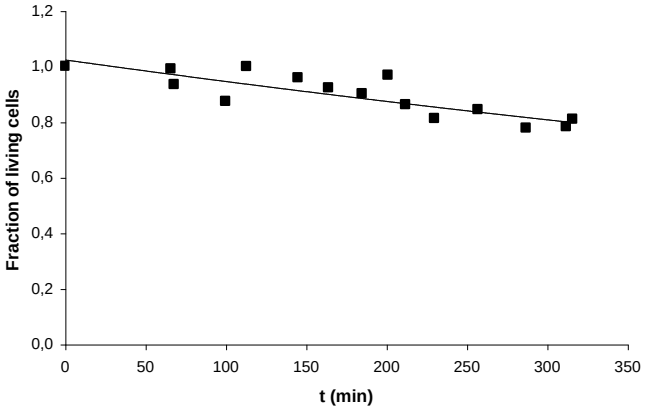

Fig. 1. Normal cell survival in YPD at 30°C. Number of dead cells is subtracted from the total number of cells and the difference is normalized to the initial number of living cells. Solid line is theoretical exponential fit. Errors are not indicated if smaller than symbols.

Effects of irradiation with accelerated protons

In proton-irradiated cells, the surviving fraction obtained with immediate plating is of $S_{IP}(p)$=27.25%. Out of the living irradiated cells only 27.25% are able to survive, to complete the first cell cycle and then divide normally for more than two times. The rest of 72.75% cells are not able to repair efficiently the radiation-induced damage during their cell cycle progression.

85 min. after irradiation the G_2/M cell fraction increases to 57% in irradiated cells as compared to the normal level of 37% in normal exponential cultures, then reaches 30% at t=135 min. and returns to the basal level at t>150 min (shown in Fig. 2).

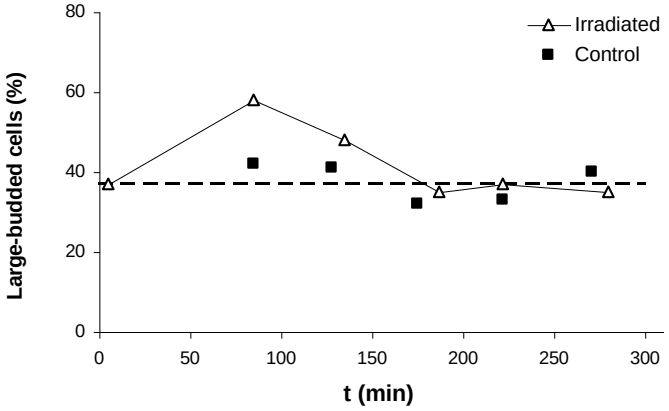

Fig. 2. Arrest at the G_2/M checkpoint after irradiation induces a transient increase in the fraction of late-G_2/M cells (% of total cells in suspension) as compared to the uniform distribution in control cells (average in control is represented by dashed line).

In conclusion, the G_2/M checkpoint is kept active during the first 2.5 hours after irradiation, since the accumulation of large budded cells in the irradiated culture corresponds to cells transiently arresting at the G2/M checkpoint [10].

As shown in Fig. 3, global cell growth appears slower than in control, with estimated mean doubling time of 99 min. as compared to 86 min. in normal cells.

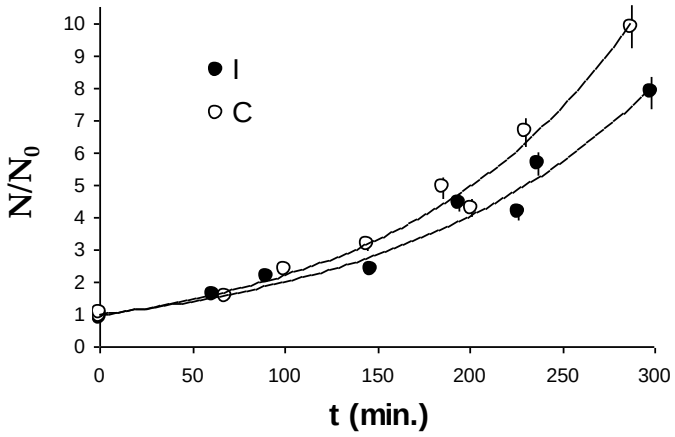

Fig. 3. Cell growth in control (C) and proton-irradiated (I) cell cultures. The number of cells in culture at an instant (N) is normalized to the initial number of cells (N_0). Solid lines are obtained by exponential theoretical fit.

98% of living irradiated cells remain viable for 155 min. after irradiation, then the fraction (=1-S_{IP}) of lethally damaged cells begin to die stochastically, yielding a best exponential fit with decay time constant of 182 min. (see Fig. 4). Radiation-induced death rate was estimated by assuming that all new born cells are viable during the first 350 min. after irradiation (i.e. during their first two cycles), so the fraction of living irradiated cells scored by the methylene-blue method comes in agreement with the plating method by extrapolating the survival curve to time values >750 min. The death rate value, 1/182 min^{-1}, suggests that after 155 min. allowed for repair, irradiated cells carrying lethal damage die on average at the end of the third division cycle. This result comes in perfect agreement with that obtained by Grundler and Abmayr [4], which shows that the approximation regarding the death of daughter cells is justified.

It is known that cells subjected to irradiation are able to recover to a certain extent when held in non-nutritive media before plating on growth media, a process called 'liquid holding recovery'. In the absence of nutrients, yeast cells stop growing by entering a highly specialized state, the G_0 stationary phase, where cells are able to repair radiation-induced damage more efficiently than during cell cycle progression. Recovery of the surviving fraction during delayed- plating treatments can be ascribed to the repair of DNA double strand breaks (dsbs) and survival obtained with delayed plating is a measure of the relative yield of DNA dsbs that cannot be repaired by the cell's repair systems [11]. In yeast cells recovery increases with time up to three days and remains stationary for the next two days, when full possible repair is completed [11].

In our experiments, irradiation with 200 Gy of protons induced in yeast cells a significant yield of irreparable damage. Survival with delayed plating was obtained as $S_{DP}(p)$=68.8%, so proton-irradiation produces irreparable damage in 31.2% living cells. The

remaining 68.8% cells consist of a group (S_{IP}=27.25% of irradiated cells) with easily repairable lesions and another group (S_{DP}-S_{IP}=41.55% of irradiated cells) with severe lesions that can only be repaired in the G_0 stationary phase.

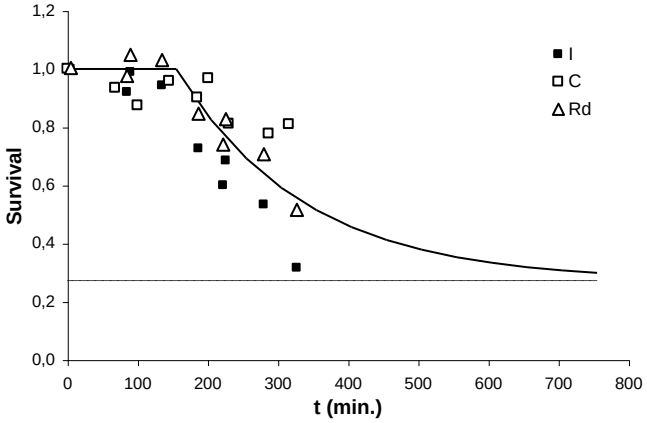

Fig. 4. Kinetics of living cell fraction in suspension. For proton-irradiated (I) and control (C) data points, number of dead cells at an instant is subtracted from the initial total number of cells, and the difference is normalized to the initial number of living cells in culture. For radiation-induced cell death (Rd) the radiation-dependent difference of survival, S(I)-S(C), is normalized to the control survival S(C). Solid line is theoretical fit to the Rd-data. Dashed line represents survival with immediate plating.

Effects of γ-radiation

At 200 Gy absorbed dose, γ-irradiated cells arrest progressively in G_2/M, with maximal fraction of large-budded cells, as high as 76% of total, reached 222 min. after irradiation. Cell proliferation is ceased for ≅130 min. following irradiation (as seen in Fig. 5), with cells accumulating at the G_2/M-checkpoint in the first cell cycle, and beginning to divide when all the radiation-induced lesions are repaired.

The mean doubling time in control and descendants of irradiated cells is obtained by exponential best fit as 94.5 min. (shown in Fig. 5). By using the growth curve and the kinetics of large-budded cell fraction of irradiated cells as determined by microscopic examination (data 'I (total)' presented in Fig. 6) we can estimate the time variation of the fraction of large-budded cells for the irradiated cells still undivided, as well as for the population of mother cells that divided at least once together with their daughters. Three additional assumptions are made:

i) the number of cells remains constant for t<140 min., as indicated by the growth curve;

ii) arrest at the G_2/M checkpoint is relieved within 140 min., since cell growth is exponential for t>140 min.

iii) the calculated G_1/S/early-G_2 cell fraction decreases linearly with time for t<140 min., so it is assumed that the rate of the S-to-G_2 passage in the first cycle is constant, calculated as 0.0125/min. from best fit to the data (see Fig. 7).

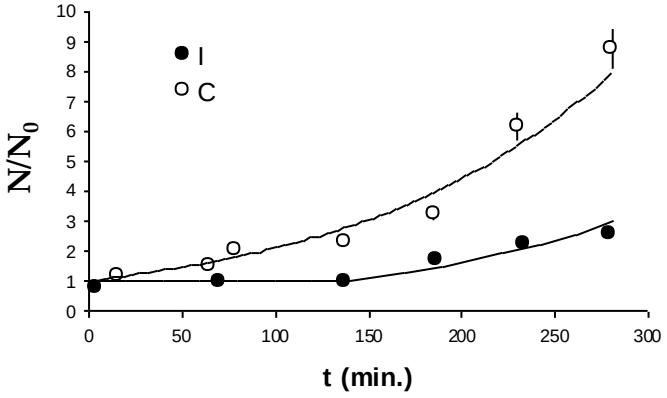

Fig. 5. Cell growth in control (C) and γ-irradiated (I) cell cultures. Solid lines are obtained by theoretical fit. Other notations as in Fig. 3.

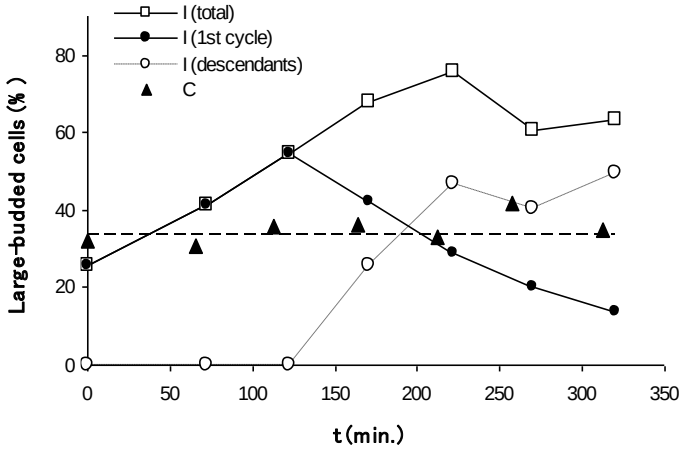

Fig. 6. Evolution of the late-G_2/M cell fraction (% of total cells in suspension) after irradiation as compared to the uniform distribution in control cells. Distribution over three cell populations is shown for irradiated cells: total G_2/M cells, 'I (total)', undivided cells, 'I (1st cycle)', and mother cells together with their daughters, 'I (descendants)'.

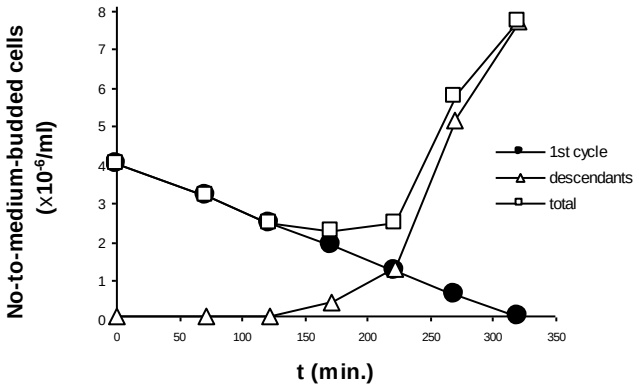

Fig. 7. Time variation of G_1-S-early G_2-cell concentration in the culture initiated with irradiated cells, determined for undivided cells ('1st cycle'), cells that underwent the first division, together with their daughters ('descendants') and total unbudded and small-to-medium-budded cells in suspension ('total').

From *ii)* and *iii)* it is evident that for t>140 min. there is no additional accumulation of cells at the end of the first cycle, so there is no increase in the number of large-budded cells in the first cycle. Quantitatively, this means that in the first cycle the rate of S-to-G_2 passage equals the rate of division.

In this way we found (as shown in Figs. 6-8) that the cells that were in the G_2-M phases at the time of irradiation divide almost synchronously after the damage is repaired during arrest at the G_2/M checkpoint, whereas cells irradiated while being in the G_1-S phases do not arrest visibly at the G_1- or S-checkpoints. After damage repair and checkpoint passage, cells begin to divide, the total number of cell in suspension increases, and the pool of cells at the end of the first cycle reduces gradually (see the curve 'I (1st cycle)' in Fig. 6).

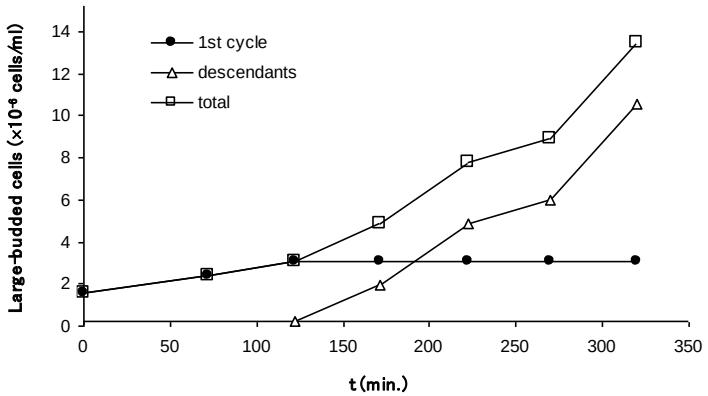

Fig. 8. Kinetics of late-G_2/M cells in the culture of irradiated cells. Legend notations as in Fig. 7.

The large-budded cell distribution over the two populations shows in Fig. 9 that 50 min. after the first division of irradiated cells there is a large proportion (87%) of G_2/M cells in the second cell cycle, which means that a major part of mother cells divided almost synchronously at t~120 min. Such an effect indicates that cells irradiated in the G_2-M phases need more time to repair their DNA breaks than do cells irradiated in the G_1-S phases, consistent with known repair mechanisms in yeast cells. Meanwhile, the G_2/M cell fraction in the first cycle increases steadily: for t≤120 min. this is due to arrest at the G_2/M checkpoint, and thereafter it is due to the continuous decrease in the number of G_1/S cells, so that at t=320 min. all cells still undivided are large-budded.

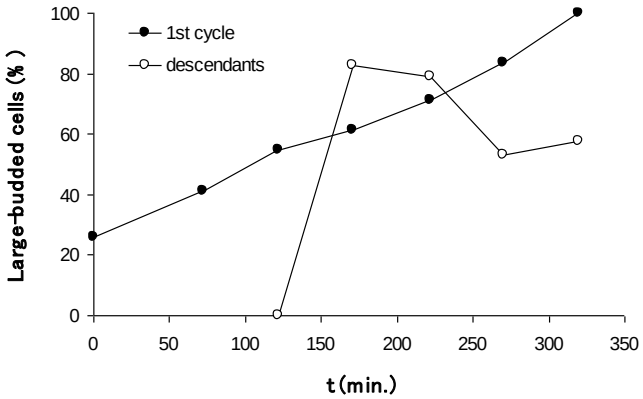

Fig. 9. Late-G_2/M cell distribution in two subpopulations: undivided irradiated cells (1st cycle) and irradiated cells that underwent the first division, together with their daughters (denoted generically as 'descendants'). The number of large-budded cells is divided to the total number of cells in each subpopulation.

During the first 220 min. after irradiation the cellular death rate in irradiated culture is comparable to the control, but begins to increase thereafter (data are summarized in Fig. 10). This means that γ-irradiated cells pass successfully the checkpoint, complete the first cycle and divide, but the radiation-induced lesions are incorrectly repaired in a large fraction of cells that die before dividing for three times, and the inherited defects in their progenitors impede them to proliferate sufficiently to produce colonies. This is reflected by the fraction of surviving cells which was obtained with immediate plating, $S_{IP}(\gamma)$ =26.7%. Interestingly, survival with delayed plating was obtained as $S_{DP}(\gamma)$ =99.9%, indicating that all damage was repaired during the stationary phase. The result is in agreement with that obtained in X-rays irradiated wild-type yeast cells, where at an exposure that induced a survival level $S_{IP}(X)\cong 27\%$, the viability was recovered up to $S_{DP}(X)>95\%$ [11].

The data presented in Fig. 10 are obtained by assuming that all descendants are viable over the experiment duration, equivalent to supposing that daughter cells do not die during their first two cell cycles. Since the result obtained in this way is in very good agreement with previous findings [4], we conclude that the approximation is justified indeed. Death of irradiated cells begins much later than in proton-irradiated cells and therefore could not be well defined in γ-irradiated cells, however it seems to have similar rate to that obtained with proton-irradiated cells.

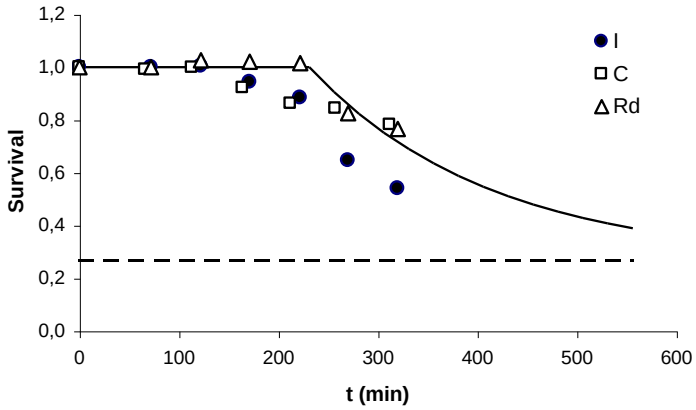

Fig. 10. Kinetics of living cell fraction in the suspension of γ-irradiated cells. Legend notations as in Fig. 4. Solid line is obtained with theoretical fit to the Rd-data, assuming the same death rate as in the case of proton-irradiation. Dashed line represents survival with immediate plating.

Comparison of γ- and proton-irradiation effects

In summary, irradiation with γ rays produces quite similar effects as proton-irradiation of yeast cells with regard to survival of cycling cells. The surviving fraction obtained with immediate plating is closely similar in the two cases, 26.7% vs. 27.25%, whereas the yield of irreparable DNA dsbs appears consistently different: 0.001 in the case of γ rays, and 0.31 with protons. It is worth mentioning that a similar value of survival, ~25%, is indicated by data obtained with wild-type *S. cerevisiae* cells irradiated with X-rays [12], which are known to produce similar effects as γ radiation.

We observed that cell kinetics is slowed down in irradiated cells, with a larger delay of the first cell cycle obtained with γ rays. Accumulation at the G_2/M checkpoint is more pronounced with γ- than with proton-radiation, with maximal fraction of large-budded cells of about 80% and 57%, reached at 220 min. and 85 min., respectively. Onset of radiation-

induced cell death is produced with a lag of 220 min. with γ rays, and 155 min. with protons (Fig. 11).

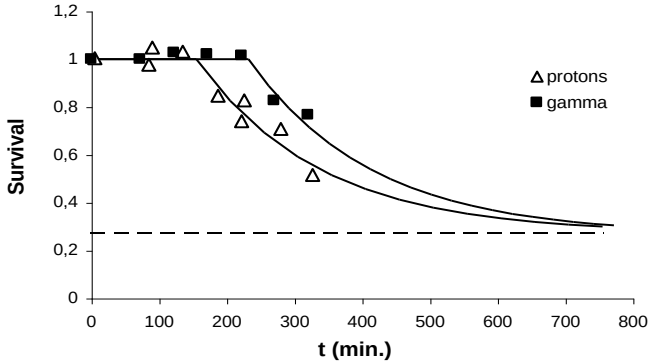

Fig. 11. Protons- and γ-radiation-induced cell death at 200 Gy. Control dead cell number is subtracted from irradiated dead cell number and the result is normalized to the initial number of living cells in the culture of irradiated cells. Dashed line represents survival with immediate plating. Solid lines are obtained by theoretical fit with stochastic cell death starting at 155 min. for protons and 222 min. for γ rays.

Radiation effects on DL

Photon emission is characterized by several independent quantities: the initial number of excited states, the probability of a state to emit a photon in one second, and the distribution of states that emit radiation with different rates. In the following we shall describe photon emission by the time dependence of the intensity of the emitted light $I(t)$ (the number of photons emitted in time unit), the total yield Y (a quantity proportional to the total number of emitted photons, or, equivalently, to the total number of excited states at t=0), the decay probability characteristic to the dominant state population, and the fraction of these dominant states relative to the total number of excited states. The latter quantities are calculated for the dominant region of emission (the first 55 μs following laser irradiation) where we approximate the decay as being exponential (explained below).

We observed an interesting effect characterized by increased light emission with wavelength $\lambda_{emitted}$ = 645 nm, by cell cultures at moments (t>120 min.) after irradiation, when the fraction of irradiated mother cells decreases considerably (<10% at the end of the experiment). This enhancement seems to be not dependent on the total fraction of G_2/M cells, since with high fractions of large-budded cells, the total yield in proton-irradiated cell culture is comparable to the control (see Figs. 2 and 12). This suggests that actually daughter cells are responsible for this effect, presumably through defects inherited from their parents, and our data with γ-irradiation indicate a possible correlation between increase in the total yield and the G_2/M descendant cells (as seen if comparing Fig. 6 to Fig. 12). Work is in progress to clarify the nature of the observed cell behaviour.

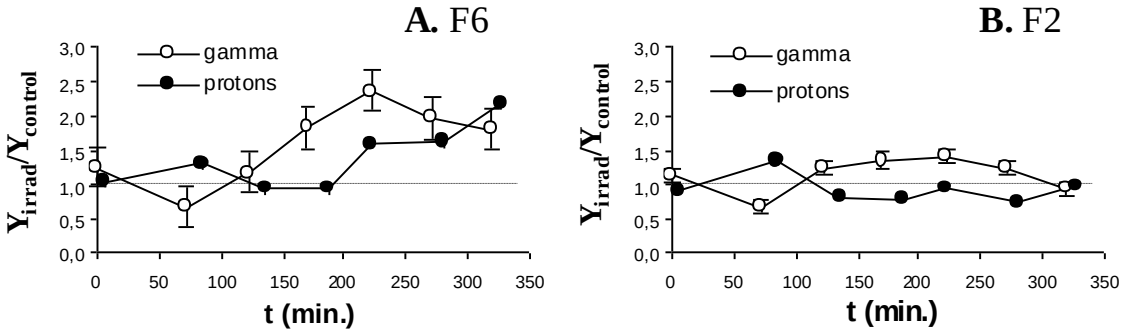

Fig. 12. Increase in total yield corresponding to the spectral components F6 ($\lambda_{emitted}$ = 645 nm) and F2 ($\lambda_{emitted}$ = 460 nm) of the light emitted by irradiated cells (Y_{irrad}) relative to the corresponding control sample ($Y_{control}$) at various moments after irradiation. Each value of the total yield is normalized to the cell number in the sample.

While the 645 nm-light emission shows on average a consistent increase relative to the control in both γ- and proton-irradiation cases (Fig. 12A), the 460 nm-light emission has a different trend, with relatively small variations around the control value for both radiation types (Fig. 12B).

In addition, clear differences appear in the decay of the light emitted by cells. In γ-irradiated cells, there is a gradual increase of the slope of the F6-photon emission curve (see Fig. 13): 5' after irradiation the decay curve of irradiated cells coincides with that obtained with control cells (not shown), then the decay becomes faster and faster as time lapses in cell cultures. The most rapid decay is obtained 222' after irradiation, which corresponds to the maximal increase in the total yield observed in Fig. 12A. The decay curves obtained for t=270' and 320', respectively, are somewhat slower (not shown) but close to that obtained at 222'.

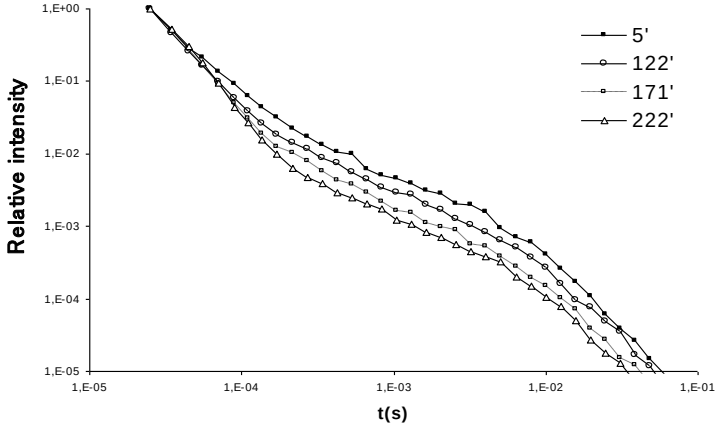

Fig. 13. Decay of light emitted with $\lambda_{emitted}$ = 645 nm by γ-irradiated cells at various moments after irradiation, which are specified in the legend. Each curve is normalized to its maximal observed value.

A similar trend is obtained with proton-irradiated cells, however the speeding up of the decay seems unsaturated even at 327', which again correlates with the data related to the increase in total yield (as seen when comparing Fig. 14 to Fig. 12A). We therefore investigated the possible correlation between the number of emitted photons and the kinetics of emission. We observed that for the F6 spectral component, with both radiation types, the higher is the total number of emitted photons, the faster is the decay.

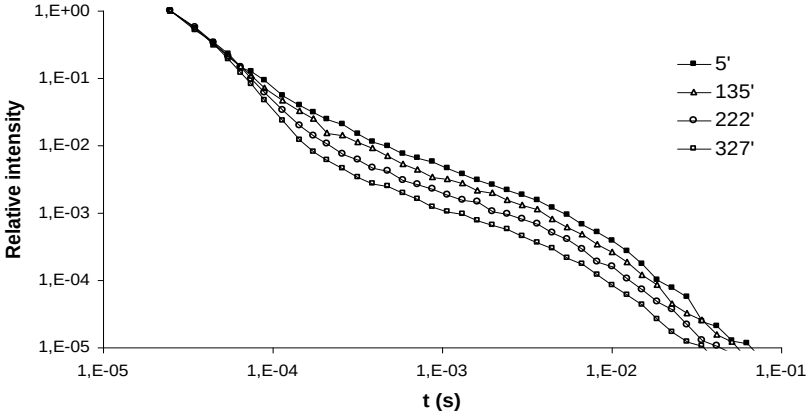

Fig. 14. Decay of light emitted with $\lambda_{emitted}$ = 645 nm by proton-irradiated cells at various moments after irradiation, specified in the legend. Each curve is normalized to its maximal observed value.

The correlation is not evident in the case of 460 nm-light emitted by γ-irradiated cells, where the kinetics of photon emission is predominantly slower than in control cells (the decay curves are not shown). Actually this kinetic behaviour appears to be in anti-correlation with the increase in intensity shown in Fig. 12B (we observed the anti-correlation also with proton-irradiated cells), however in this case the deviations from the control level are relatively small and thus make the analysis inconclusive.

In order to quantify these effects, we compared the decay of photon emission in irradiated to control samples. The initial decay of each intensity curve $I(t)$ is well fitted by an exponential function of time (r^2 between 0.978 and 0.999, not shown), which gives the decay rate of the dominant state population in that region. Assuming that there are different classes of excited states that decay with different rates, we obtain for irradiated and control samples, respectively:

$$N_{0i} = N_{10i} + N_{20i} + ... = \alpha_{1i} N_{0i} + \alpha_{2i} N_{0i} + ...$$
$$N_{0c} = N_{10c} + N_{20c} + ... = \alpha_{1c} N_{0c} + \alpha_{2c} N_{0c} + ...$$

where N_0 is the total number of excited states at t=0, and N_{j0} the number of states corresponding to population j (j=1,2,…) at t=0, and α_j the fraction of j-type states, with $\sum_j \alpha_j = 1$. All states in a certain population j are characterized by the decay probability per time unit, P_j. Then, for each state population, the number of states decreases according to the relation:

$$\frac{dN_j(t)}{dt} = -P_j N_j(t)$$

which gives the time dependence of the intensity of emitted light as

$$I(t) = -\sum_j \frac{dN_j}{dt} = -N_0 \sum_j \alpha_j P_j \exp(-P_j t)$$

For the dominant region of the spectrum (the first 55 μs following laser irradiation) the dependence of the intensities I_i vs. I_c can be considered linear (r^2 between 0.98 and 0.999, not shown). For t sufficiently small the dependence I_i vs. I_c is not linear unless the dominant states '1' have the same decay probability ($P_{1i} = P_{1c}$). Indeed, in the initial region with exponential decay of the intensity we may approximate $I(t)$ as the contribution of states from population '1', so we obtain

$$\frac{I_i(t)}{I_c(t)} \cong \frac{N_{0i}\alpha_{1i}P_{1i}\exp(-P_{1i}t)}{N_{0c}\alpha_{1c}P_{1c}\exp(-P_{1c}t)}$$

It follows then that I_i becomes linear on I_c when $P_{1i} = P_{1c}$. This means that in both control and irradiated cells the dominant states are of the same type, i.e. originate from the same cellular components. So, when the decay curves are normalized to the initial number of states N_0, the resulting differences in the decay kinetics are due to the differences in the state fractions, and we have

$$\frac{I_i(t)/N_{0i}}{I_c(t)/N_{0c}} \cong \frac{\alpha_{1i}}{\alpha_{1c}}$$

We first extracted the value of the ratio α_{1i}/α_{1c} from the linear fit $I_i/N_{0i}=f(I_c/N_{0c})$ obtained for $t<55$ μs and then calculated separately the values α_{1i} and α_{1c} for the region of exponential decay ($t<t_1$, with $t_1=55$ μs; here the intensity decreases more than 50 times from the estimated value at $t=0$), by considering that

$$\alpha_1 \cong \frac{1}{N_0}\int_0^{t_1} I(t)dt \text{, where } N_0 = \int_0^{\infty} I(t)dt$$

Both methods give extremely close values for the α_{1i}/α_{1c} ratios.

We found that in both γ- and proton-irradiated cells the fraction of type '1r'-states (the dominant class of states that emit red light, with $\lambda_{emitted}$ = 645 nm) increases with up to 40-45% of its normal value (Fig. 15A), meaning that both radiations induce the appearance of a larger proportion of type '1r'-states.

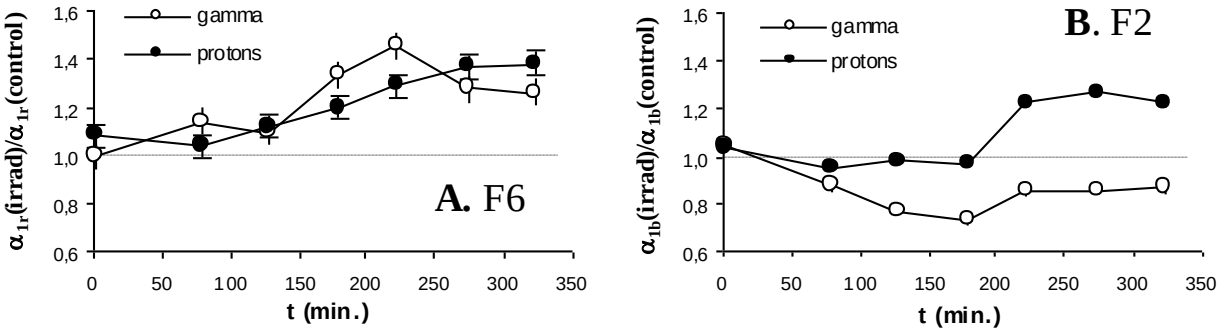

Fig. 15. Radiation-induced variations in the fraction α_1 of the dominant population of excited states that decay by F6- (**A**) or F2- (**B**) light emission.

Meanwhile, γ-rays induce a reduction with up to 27% of the normal value in the proportion of type '1b'-states (the dominant class of states that emit blue light, with $\lambda_{emitted}$ = 460 nm), whereas protons increase this fraction with up to 30% (Fig. 15B).

In order to see whether these variations are due either to the total number N_{10} of '1'-states or to the number of other type ('2', '3'…) states, we calculated the differences in the total number of states N_0 and in the number N_{10} induced by irradiation. The results shown in Fig. 16 indicate that the induction - by both radiation types - of more excited states that emit red light is more than 60% due to an increase of the number of type '1r' states.

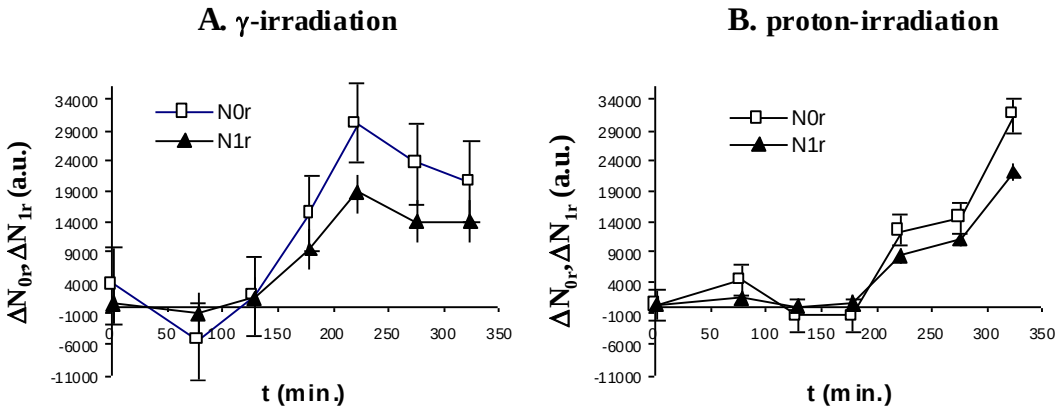

Fig. 16. Radiation-induced variations in the number of total states (ΔN_{0r}) and number of states in the dominant population (ΔN_{1r}) of states that decay by 645 nm-light emission, calculated as the difference between the respective number in irradiated and that in control cells. All represented quantities equal their actual value multiplied by the same amplification factor.

Within the population of states that emit blue light the number of '1b'-states seems unaffected (Fig. 17) by both radiations, whereas the total number of states varies in opposite ways in the two cases. These results indicate that protons and γ-rays have opposite effects on minor populations but do not affect the major population of states emitting blue light.

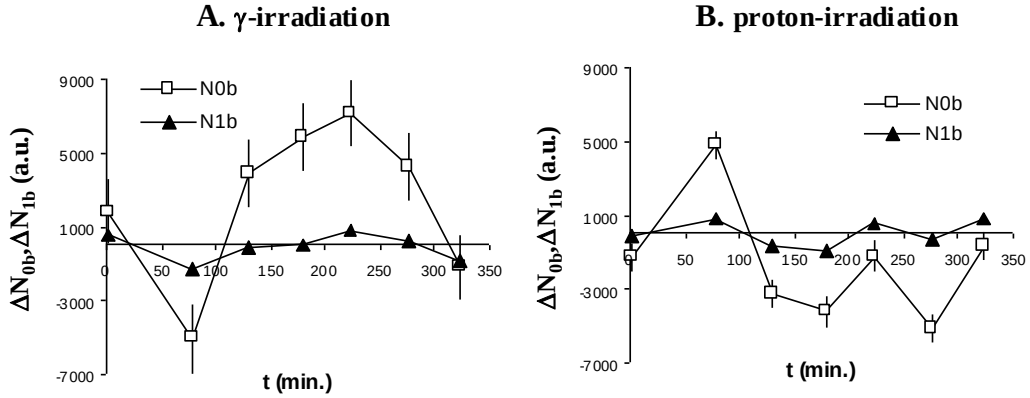

Fig. 17. Radiation-induced variations in the number of total states (ΔN_{0b}) and number of states in the dominant population (ΔN_{1b}) of states that decay by 460 nm-light emission, calculated as the difference between the respective number in irradiated and control cells. The amplification factor is the same as in Fig. 16.

The probabilities of photon emission characterizing the major populations of red- and blue-light emitting, '1r'- and '1b'-states, have quite close values (as derived from the exponential fit to the initial decay of the intensity curves $I(t)$), with a ratio P_{1r}/P_{1b}=1.13. The identification of the cellular structures that define these different classes of light-emitting states is currently under investigation by means of applying various drug treatments that affect different cellular targets.

Finally, the correlation between the rapidity of light emission and the total initial number of excited states, observed for the F6 component, can be explained by the correlation between the increase in the fraction of '1r'-states and the increase in N_{0r}, corroborated by the fact that the major population of states has a higher decay rate than do the other classes of states. For example, an estimation of the decay rate in the second exponential region of the spectrum (the fit has r^2>0.969) shows that P_2 is 7-8 times lower than P_1, and the fraction of

'2'-states is $\alpha_2 \cong 0.1$, as compared to $\alpha_1 \cong 0.3$-0.6. In this way, if the proportion of '1r'-states increases, the decay region dominated by these states is prolonged by fast decay of the supplementary '1r'-states and the slower contribution of the other type states appears later than in the normal case. The results showing the correlation between the data in Fig. 12A, 13 and 14 are summarized in Fig. 18.

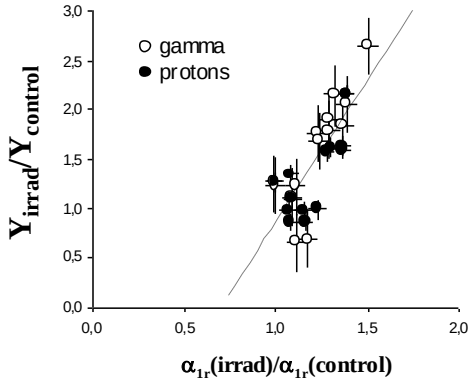

Fig. 18. Correlation between the total yield of emitted light and the fraction of states in the dominant population of states that decay by 645 nm-light emission. The correlation Pearson factor is 0.788. Dashed line is obtained with linear best fit to all data points.

Discussion

We characterize several effects of 200 Gy proton- and, respectively, γ-irradiation on wild-type *S. cerevisiae* yeast cells. From our results, summarized in Table I, we conclude that γ rays produce DNA lesions that arrest cells at the G_2/M checkpoint a longer time than with protons, possibly because the density of the ionization is uniform with electromagnetic radiation and more DNA breaks are produced. However, the relative yield of lethal damage (double strand breaks that cannot be repaired during cell cycle progression), appears closely similar in both radiation types, but injury is more severe in the proton-radiation case, since the relative yield of irreparable alterations (dsbs that cannot be repaired in either G_0 or during cell cycle progression) is 0.31 as compared to 0.001 in the case of γ rays. Meanwhile, the relative yield of severe lesions (which can only be repaired in the G_0 stationary phase) is 0.417 with protons and 0.732 with γ rays. These results point to the different effects proton- and γ-radiations might have on the viability of human specialized cells resting in G_0, such as unstimulated lymphocytes, and suggest that RBE for protons is consistently higher with resting than with cycling cells.

We also found that proton- and γ-radiations have similar effects on the states that decay by emitting red (645 nm) light, however with a delay of about 100 min. in the case of proton-irradiation as compared to the case of γ-irradiation. In both cases there is a consistent (up to ≅2.5-fold) increase in the total number of excited states, of which more than 60% is due to the increase in the number of states that decay at high rate. The fraction of this dominant state population increases as well after irradiation, leading to the observed correlation between the total yield of emitted red light and the decay rapidity.

Differentiated radiation effects are observed in the states that decay by emitting blue (460 nm) light, where the dominant state population, characterized by high decay rate,

appears to be unaffected by either radiation type, while the populations of states with slower decay rate are affected in opposite ways by protons and γ-rays, showing out-of-phase kinetics. Further investigations are needed to identify the cellular structures that define these two different classes of states which appear differentially affected by protons and γ-rays. As a first step, we are currently studying the possible implication of the cytoskeleton and mitochondria, with the use of various chemical agents that act specifically on these cellular components.

Acknowledgements

One of us (I. B.) addresses special thanks Professor C. Ganea and Professor E. Katona for continuous support and advice during this project. I. B. and V. B. gratefully acknowledge the warm hospitality and stimulating scientific environment at Laboratori Nazionali del Sud, Catania, Italy. The authors thank Carla Motta for valuable assistance in cell culture preparation and analysis.

References

1. LONGHESE, M.P., CLERICI, M., AND LUCCHINI, G. The S-phase checkpoint and its regulation in *Saccharomyces cerevisiae*. *Mutation Res*. **532**:41–58.
2. SIEDE, W. Cell cycle arrest in response to DNA damage: lessons from yeast. *Mutation Res*. **337**:73-84 (1995).
3. ANDREASSEN, P.R., LOHEZ, O.D., AND MARGOLIS, R.L. G_2 and spindle assembly checkpoint adaptation, and tetraploidy arrest: implications for intrinsic and chemically induced genomic instability. *Mutation Res*. **532**:245–253 (2003).
4. GRUNDLER, W. AND ABMAYR, W. Differential inactivation analysis of diploid yeast exposed to radiation of various LET. I. Computerized single-cell observation and preliminary application to X-ray treated Saccharomyces cerevisiae. *Radiat. Res.* **94**:464-79 (1983).
5. GALANIN, M.D. 1996. Luminescence of Molecules and Crystals. Cambridge International Science Publishing, Cambridge
6. SCORDINO A, TRIGLIA A, MUSUMECI F. Analougus features of delayed luminescence from *Acetabularia acetabulum* and some solid state systems. J Photochem Photobiol B 56: 181-186 (2000).
7. IIDA , H., YAGAWA, Y. AND ANRAKU, Y. Cell cycle control by Ca^{2+} in Saccharomyces cerevisiae. *J. Biol. Chem.* **265**:13391-13399 (1990).
8. MULLER, E.G.D. Thioredoxin deficiency in yeast prolongs S phase and shortens the G1 interval of the cell cycle. *J. Biol. Chem.* **266**:9194-9202 (1991).
9. TUDISCO S, MUSUMECI F, SCORDINO A, PRIVITERA G. Advanced research equipment for fast ultraweak luminescence analysis. *Rev Sci Inst* **74**: 4485-4490 2003.
10. VIALARD., J.E., GILBERT, C.S., GREEN, C.M., AND LOWNDES, N.F.. The budding yeast Rad9 checkpoint protein is subjected to Mec1/Tel1-dependent hyperphosphorylation and interacts with Rad53 after DNA damage. *EMBO J.* **17**:5679-5688 (1998).

11. USAMI, N., YOKOYA, A., ISHIZAKA, S., AND KOBAYASHI, K. Reparability of lethal lesions produced by phosphorus photoabsorbtion in yeast cells. *J. Radiat. Res.* **42** :317-331 (2001).
12. XU, Z. AND NORRIS, D. The *SFP1* gene product of *Saccharomyces cerevisiae* regulates G_2/M transitions during the mitotic cell cycle and DNA-damage response. *Genetics* **150**:1419-1428 (1998).